Fatigue Crack Propagation in Butt Welds Containing Joint Penetration Defects

Experiments on low carbon steel indicate a crack initiation period of about half the total fatigue life, the latter being severely reduced by joint penetration defects

BY F. V. LAWRENCE AND W. H. MUNSE

ABSTRACT. Fatigue tests have been conducted on low carbon steel butt welds containing joint penetration defects (less than complete joint penetration). The growth of fatigue cracks from simulated penetration defects was monitored by radiography. These measurements allowed the total fatigue life to be separated into periods of crack initiation and crack propagation.

It was found that the rate of crack growth conformed to the expression:

$$\frac{da}{dN} = 0.27 \times 10^{-13} (\Delta K)^{5.8}$$

The initiation period was found to occupy approximately one half of the total fatigue life and consists of the cycles necessary to shake down the residual stresses in the weld and to form the penetration defect into an active fatigue crack.

F. V. LAWRENCE is Assistant Professor, Metallurgical and Civil Engineering and W. H. MUNSE is Professor of Civil Engineering, University of Illinois, Urbana

Introduction

The fatigue life of flawed materials such as weldments containing internal defects may be separated into two portions: that fraction of the life in which flaws sharpen to become active fatigue cracks (initiation), and that fraction in which the sharpened cracks steadily enlarge until fracture occurs (propagation).

The propagation portion of the fatigue life has been extensively studied. Paris[1] found that the rate of crack growth per cycle was proportional to a power of the range in stress intensity factor of the propagating crack. Recent studies have confirmed the validity of this concept for a wide range of materials.[2-6]

The initiation period has proven to be more difficult to describe or measure. Furthermore, there are no suitable theories available which allow quantitative estimates to be made of the life spent in initiation. It is often conservatively assumed that the initiation period does not exist and that all life is spent in crack propagation; however, this philosophy is not justified on the basis of the observed data.

Previous fatigue studies by the authors in weldments in the HY-series steels[7-9] have suggested that a considerable portion of the fatigue life, possibly as much as one-half, is spent in crack initiation (or undetected crack growth).

In the current study, the authors have investigated the fraction of life spent in crack propagation in A36 low carbon steel weldments.[10] The principal experimental method involved the radiographic monitoring of internal crack growth from a simulated joint penetration defect. The results of these experiments provided crack growth data which can be compared with the theoretically determined fatigue crack growth.

Weld Fabrication and Fatigue Testing

The specimens were fabricated from ¾ in. (19mm) thickness ASTM A36 steel plate. The welding electrode was a 1/16 in. (1.6 mm) diam base wire equivalent to E70 grade electrodes with a minimum ultimate tensile strength of 70 ksi (482.6 N/mm²). The mechanical properties of the base metal and the chemical analysis of the base metal and electrode are listed in Table 1.

The plate segments were joined with a partial-penetration double-U butt weld using gas metal-arc (GMA) welding with A-5% O_2 shielding gas.

Table 1—Mechanical Properties and Chemical Composition

ASTM-A36 Mechanical Properties

Yield Point	41,000 psi (283.5 N/mm²)
Tensile Strength	70,900 psi (488 N/mm²)
Elongation in 8 in. (315 mm)	27%

Chemical Composition, wt %

Material	C	Mn	P	S	Si
A36 base metal	0.23	0.9	0.015	0.03	—
E70 1/16 in. (1.6mm) wire	0.09	1.0	0.017	0.024	0.45

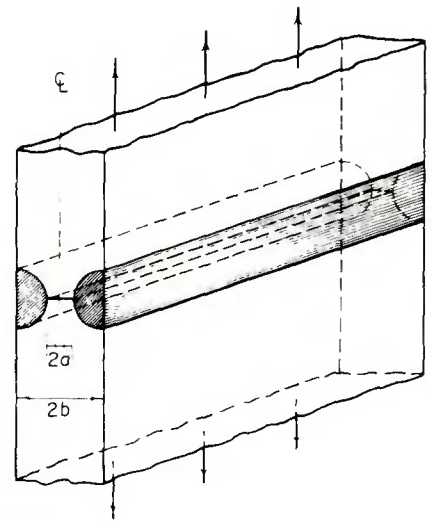

Fig. 1—Partial penetration butt weld showing unwelded depth (2a) representing a penetration defect in a fatigue loaded joint

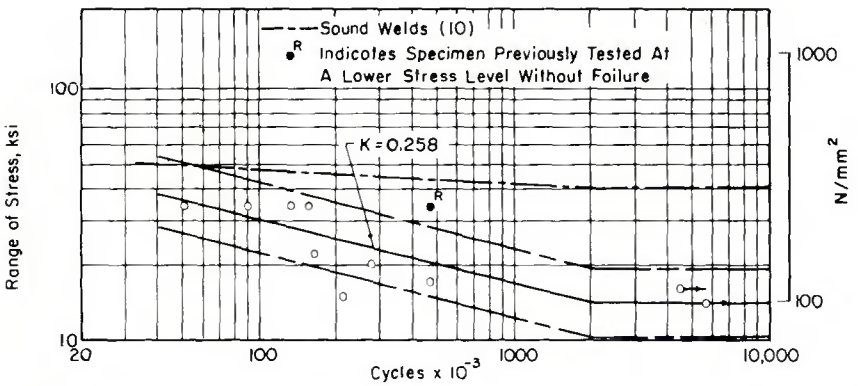

Fig. 2 — S-N curve for sound welds and weld containing 3/16-in. (4.8 mm) lack of penetration[10]

By proper manipulation of the welding parameters, a 3/16-in. (4.8 mm) deep penetration void persisting for the whole length of the weld could be produced (see Fig. 1.). The penetration defect created in this manner could not be detected radiographically; the compressive residual stresses in the center of the weld were sufficient to close tightly the unwelded depth of joint. To verify the absence of complete joint penetration prior to testing, it was necessary to look at polished sections or to perform tensile or side bend tests on sections of the weld.

After the specimens were machined to shape and their weld reinforcement removed, they were mounted in a 50 kip (222.4 kN) Illinois lever-type fatigue testing machine and tested to failure under axial loadings at a rate of 300 cpm in ambient conditions. Eleven tests on such penetration defects were performed.

Three tests were periodically interrputed to allow radiographs to be taken of the penetration void and thus determine the amount of crack growth from the defect. The radiographs were taken parallel to the axis of the weld so that the penetration defect could be imaged in profile. The width of the specimens was, therefore, necessarily limited to 1.5 in. to permit the x-rays to penetrate the full length of the weld. Crack advances of 0.01 in. ($\Delta a = 0.005$ in.) could be detected and measured.

Upon completion of the tests, the initial flaw dimensions were verified directly on the fracture surfaces.

Results of Fatigue Tests and Crack Propagation Studies

The results of all fatigue tests are listed in Table 2. The resulting S-N curve computed using a least squares fit is shown in Fig. 2 with limits of two standard deviations. The S-N data for sound, defect-free welds are also plotted.[10] It can be seen that a 3/16 in. (4.8 mm) penetration void greatly affects the fatigue behavior of the weldments. The stress range at the fatigue limit (assumed to be approximately 2×10^6 cycles) was affected most, being 40 ksi (276 N/mm²) in the case of a sound weld and 15 ksi (107 N/mm²) for welds containing a 3/16 in. (4.8 mm) deep penetration defect.

The measured variation of crack length with cycles for specimens LP1-2-1, LP1-2-4, and LP1-2-5 are plotted

Table 2 — Results of Fatigue Tests on Welded Specimens Containing 3/16-in. Joint Penetration Defect[10]

Specimen number	Stress range;[(a)] ksi (N/mm²)	Stress ratio	Life in thousands of cycles, (N_T)	Crack propagation life in thousands of cycles, (N_{pm})	Defect size, in. (mm) ($2a_n$)	Specimen thickness, in. (mm) (2b)
LP1-2-1	34.0 (234.4)	+0.056	133.1	77.1	.142 (3.60)	.704 (17.86)
LP1-2-2	20.0 (137.9)	+0.445	272.6	(b)	.175 (4.45)	.691 (17.55)
LP1-2-3	16.9 (116.5)	+0.531	464.1	(b)	.174 (4.42)	.687 (17.45)
LP1-2-4	34.0 (234.4)	+0.056	157.0	61.8	.167 (4.25)	.694 (17.60)
LP1-2-5	34.0 (234.5)	+0.056	90.8	40.3	.160 (4.06)	.704 (17.86)
LP2-6-6	35.9 (257.5)	+0.056	50.2	(b)	.150 (3.81)	.709 (18.00)
LP2-6-7	16.0 (110.3)	+0.111	4500.0+	(b)	.162 (4.11)	.713 (18.10)
LP2-6-8	22.0 (151.7)	+0.389	167.0	(b)	.205 (5.10)	.701 (17.80)
LP2-6-9	14.0 (96.5)	+0.613	5700.7+	(b)	.240 (6.10)	.690 (17.50)
LP2-6-9A	34.0 (234.4)	+0.056	469.9	(b)	.240 (6.10)	.690 (17.50)
LP2-6-10	15.0 (103.4)	+0.584	216.8	(b)	.237 (6.02)	.691 (17.55)

(a) Based on gross cross section
(b) Propagation life not determined

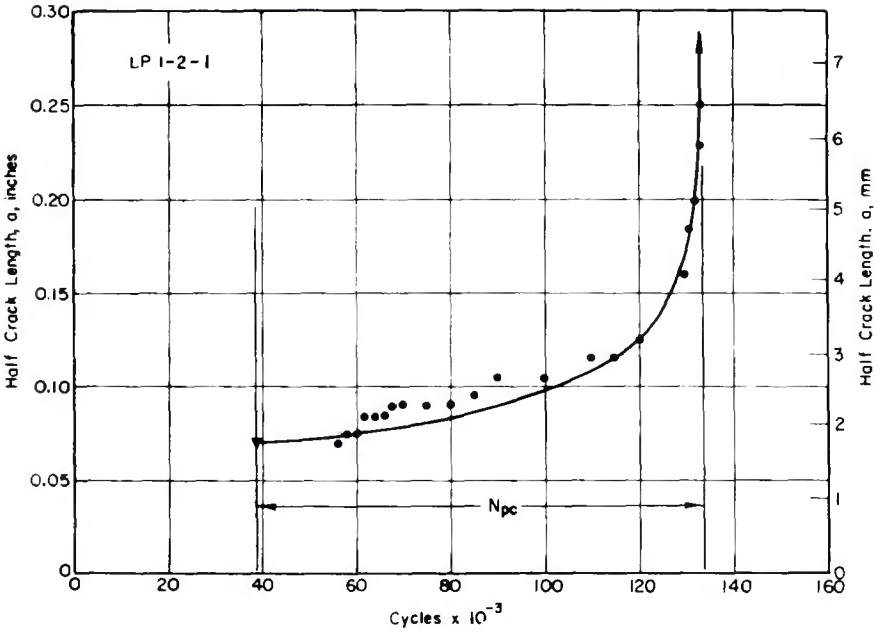

Fig. 3 — Half crack length versus cycles for specimen LP1-2-1. Points are the measured data. Curve is calculated

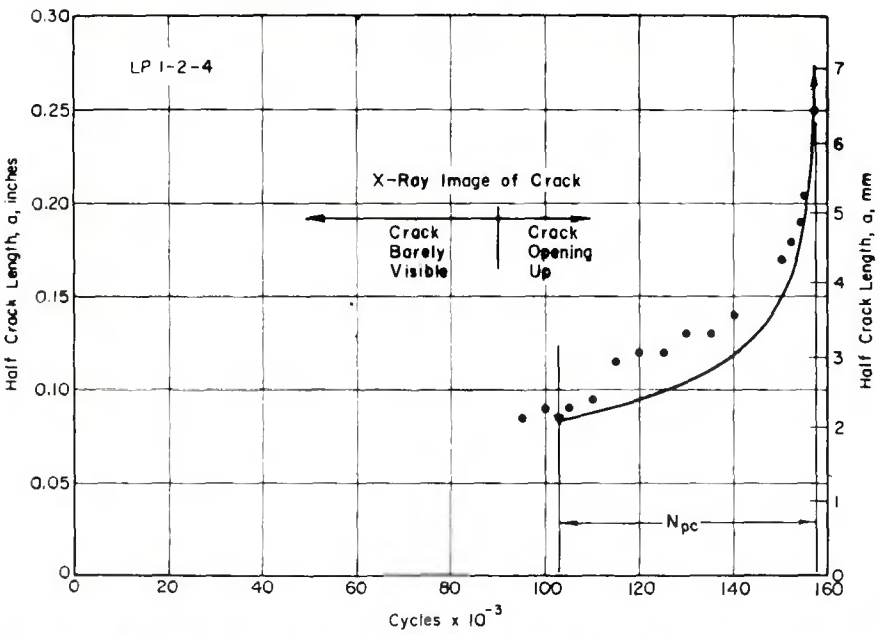

Fig. 4 — Half crack length versus cycles for specimen LP1-2-4. Points are the measured data. Curve is calculated

in Figs. 3, 4, and 5 respectively. The point at which crack propagation began was determined from periodic radiographs taken during the tests. During the early stages of a test, the penetration void remained invisible, even though the specimen was radiographed while under peak (tensile) loads. Gradually, as the residual stresses apparently shook down, the penetration void became visible and just prior to measurable crack growth became very well defined due to rapidly increasing crack opening displacements as evidenced by ever sharper x-ray images (see Fig. 4).

Smooth curves (not shown) were drawn through the data, and the slope of the curves (da/dN) at particular values of half crack length (a_i) were measured. The value of the range in stress intensity factor (ΔK) was calculated for the geometry shown in Fig. 1 from the relation:[11]

$$\Delta K = \Delta\sigma\sqrt{\pi a}\ \sec\left(\frac{\pi a}{2b}\right)^{1/2}$$

where:

ΔK = range in stress intensity factor

$\Delta\sigma$ = stress range to which the member is subjected

a = half crack length

2b = specimen thickness

With ΔK values computed using Eq. 1, a plot of ΔK versus da/dN was constructed as shown in Fig. 6. A best fit curve was computed using the method of least squares, and the two standard deviation limits are indicated.

The equation for the straight line representing the data is:

$$\frac{da}{dN} = C\ (\Delta K)^m \qquad (2)$$

where:

m, C = material constants

The values of m and C determined for the data presented in Fig. 6 are: m = 5.8 and C = 0.269 × 10^{-13} so that for the data in Fig. 6:

$$\frac{da}{dN} = 0.269 \times 10^{-13}\ (\Delta K)^{5.8}* \qquad (3)$$

Calculated Crack Propagation Lives

From Eq. 2, the following can be obtained.

$$\int_{a_o}^{a_f} \frac{da}{C\ (\Delta K)^m} = \int_{o}^{N_f} dN \qquad (4)$$

Substituting ΔK from Eq. 1 and writing Eq. 4 in terms of finite differences:

$$N_{pc} = \sum_{a_o}^{a_f} \frac{1}{C}\left(\frac{\cos\frac{\pi a}{2b}}{\Delta\sigma\sqrt{\pi a}}\right)^m \Delta a$$

where:

a_f = half crack length at failure

a_o = initial half crack length

N_{pc} = crack propagation life (calculated)

Δa = finite advance of crack

Using values of C and m from Fig. 6, the initial size of the penetration void (a_o) measured on the fracture surface and the relationship of Eq. 5, the number of cycles spent in crack propagation was computed for specimens LP1-2-1, LP1-2-4, and LP1-2-5. Table 3 gives a comparison of measured and calculated crack propagation lives, and the calculated crack propagation curves versus cycles are plotted in Figs. 3, 4, and 5 as solid lines. The calculated crack length versus cycle curves are in reasonable agreement with the measured data,

*See Table 4

and the calculated cycles of crack propagation N_{pc} differ from the measured values by an average of about 30 percent.

There are several possible sources for this error, which is not large considering the uncertainties in the measurements. There are uncertainties in defining the time at which cracks begin to propagate (resolution of radiographic measurement at ±0.005 in. [0.127 mm]). This error could result in an error in crack propagation life of about 15,000 cycles, or about 25 percent of the average measured crack propagation life, N_{pm}, depending upon the frequency of measurement and the sensitivity of the radiographs. With the stresses and initial flaw sizes used a similar uncertainty in life exists for the direct measurement of the size of initial flaw, ±0.005 in. (0.127 mm). Consequently, the agreement between the measured and calculated crack propagation lives (N_{pm} and N_{pc}) is considered to be good.

Figure 7 provides a further comparison of the measured and calculated propagation lives. The total lives of all specimens tested at a 34 ksi stress range, as well as the propagation lives, have been plotted in this diagram, and it can be seen that the calculated propagation life N_{pc} provides a very good lower bound estimate of the total fatigue life. However, such estimates of total life are reliable only when an accurate description of the initial flaw sizes and appropriate values for the constants C and m are available.

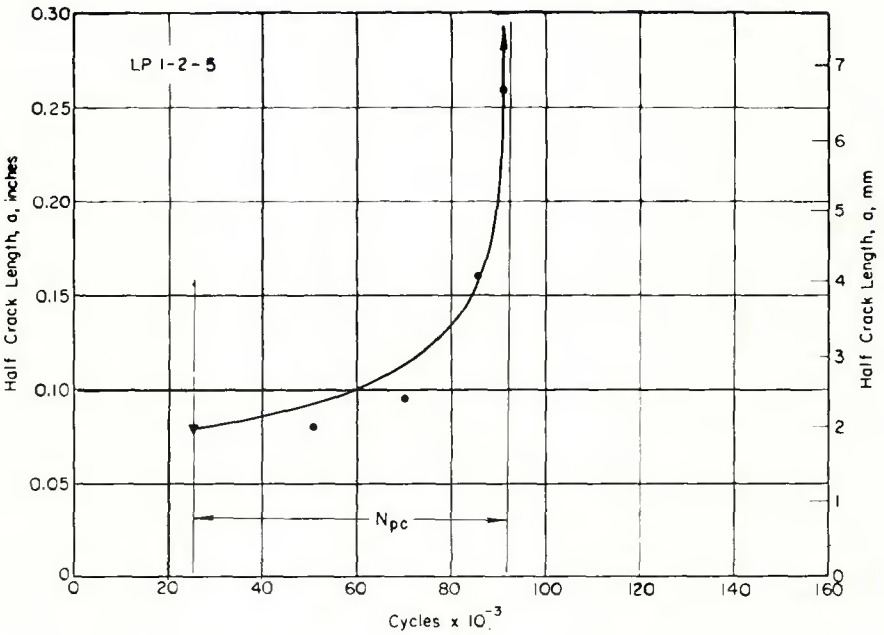

Fig. 5 — Half crack length versus cycles for specimen LP1-2-5. Points are the measured data. Curve is calculated

Table 3 — Comparison of Measured and Calculated Crack Propagation Lives

Specimen Number	a_o in. (mm)	Total Life, (N_T) cycles ×10⁻³	Crack propagation life, measured, (N_{pm}) cycles ×10⁻³	Crack propagation life, calculated, (N_{pc}) cycles × 10⁻³	Initiation period, measured, (N_i) cycles × 10⁻³
LP1-2-1	.07 (1.78)	133.1	77.1	94.4	56.0
LP1-2-4	.085 (2.16)	157.0	61.8	54.1	95.2
LP1-2-5	.08 (2.01)	90.8	40.3	65.4	50.5

Initiation Period

From the measured and calculated crack propagation lives, it appears that about one half of the total life N_T was spent in crack initiation and about one half in propagation. The assumption that the total fatigue life N_T was spent in crack propagation would lead to back calculated crack sizes smaller than those observed (0.06 in. [1.52 mm] versus 0.07 in. [1.78 mm] observed for specimen LP1-2-1). This fact coupled with the

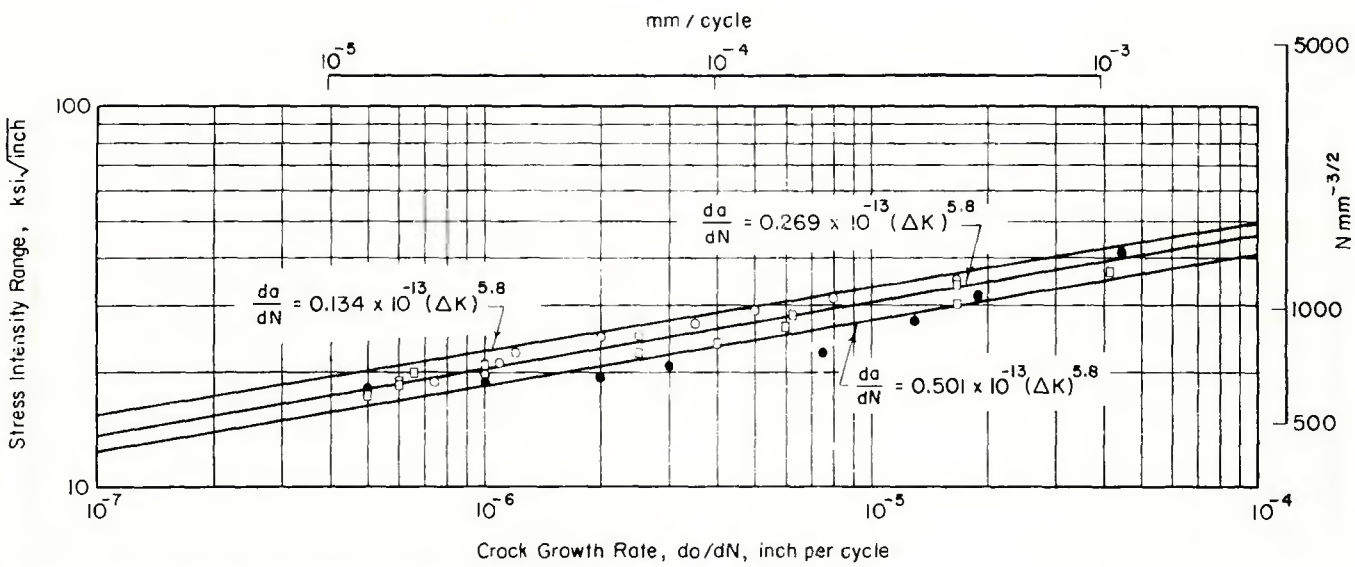

Fig. 6 — Stress intensity factor range versus crack growth rate

Table 4—Comparison of Crack Growth Parameters (For ΔK in ksi$\sqrt{\text{inch}}$ and da/dN in inch/cycle)

Material	m	C
E70 weld metal (as welded)	5.8	0.27×10^{-13}
A36 [a]	3.3	0.1×10^{-9}
Ferrite pearlite steel average [a]	3.0	0.36×10^{-9}
Martensitic steel average [a]	2.25	0.66×10^{-8}

(a) Data from Barsom[3]

observed gradual development of a crack opening displacement indicates that a significant fraction of the fatigue life is spent in initiating the crack.

The manner in which cracks form to become active fatigue cracks must be more fully understood before this initiation period can be predicted. Moreover, the period spent in crack initiation in welded joints containing centrally located internal flaws will be comprised of both the aforementioned crack forming phenomena and the number of cycles required to "shake down" the high residual compressive stresses in the vicinity of such flaws.

Comparison with Crack Growth Data from Other Sources

Because internal weld defects propagate principally through weld metal and often heat-affected base metal, the appropriate values of C and m to be used in any calculation of fatigue crack propagation life would be those for the weld metal and not the base metal. As can be seen in Table 4 and Fig. 8, there is an appreciable difference between the values of C and m measured in this study for propagation through weld metal and the values reported for ASTM A36 steel. The effect of this difference is most pronounced in the low ΔK region, the region which is most

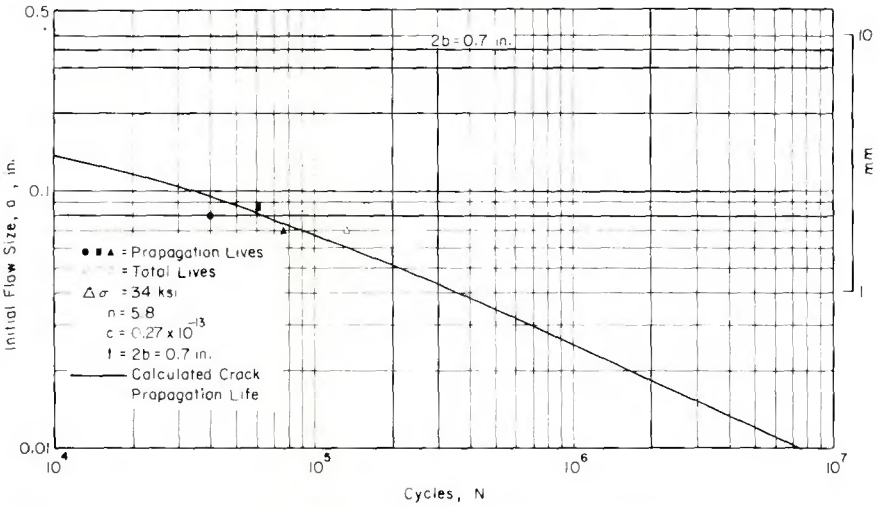

Fig. 7 — Initial flaw size versus fatigue life for a 34 ksi (232 N/mm²) stress cycle

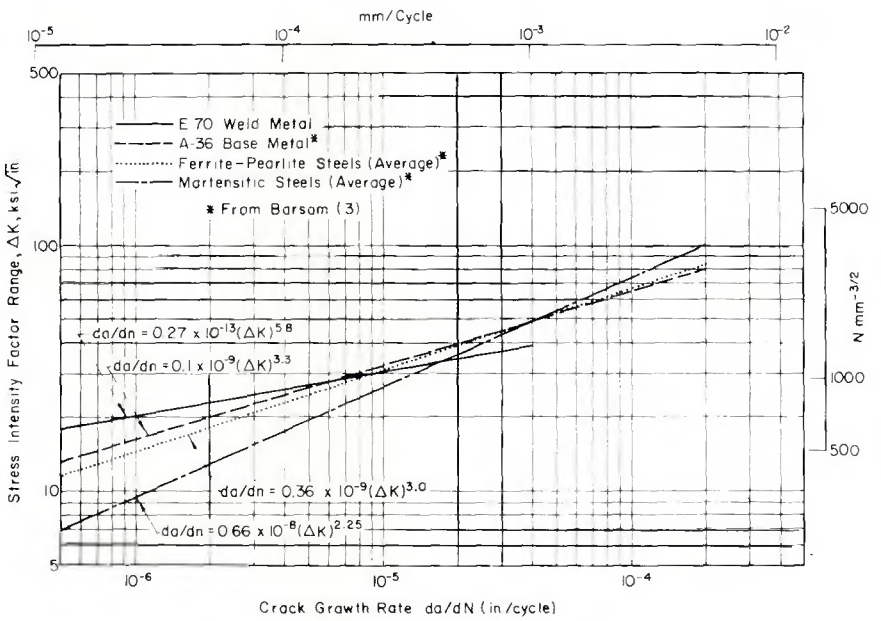

Fig. 8 — Comparison of fatigue crack propagation data

significant in terms of the fatigue life of a member. The reason for this difference is most likely due to compressive residual stresses at the root of the weld in the vicinity of the joint penetration defect. These compres-

(Continued on p. 232)

Table 5 — Comparison of Calculated Crack Propagation Lives

Specimen number	Measured total life, $N_T\times10^{-3}$	Measured crack propagation life, $N_{pm}\times10^{-3}$	Calculated Crack Propagation Life, Cycles $N_{pc}\times10^{-3}$: E70 weld metal $C=0.27\times10^{-13}$ m=5.8	A36 steel [a] $C=0.1\times10^{-9}$ m=3.3	Pearlitic steels (avg) [a] $C=0.36\times10^{-9}$ m=3.0	Martensitic steels (avg) [a] $C=0.66\times10^{-8}$ m=2.25
LP1-2-1	133.1	77.1	94.4	49.2	34.7	20.0
LP1-2-4	157.0	61.8	54.1	35.9	26.0	15.9
LP1-2-5	90.8	40.3	65.4	40.2	28.8	7.3

(a) Data from Barsom[3]